Quantum confinement and surface chemistry of 0.8–1.6 nm hydrosilylated silicon nanocrystals*

Pi Xiao-Dong(皮孝东), Wang Rong(王 蓉), and Yang De-Ren(杨德仁)†

State Key Laboratory of Silicon Materials and Department of Materials Science and Engineering, Zhejiang University, Hangzhou 310027, *China*

(Received 24 September 2013; revised manuscript received 9 January 2014; published online 15 May 2014)

In the framework of density functional theory (DFT), we have studied the electronic properties of alkene/alkyne-hydrosilylated silicon nanocrystals (Si NCs) in the size range from 0.8 nm to 1.6 nm. Among the alkenes with all kinds of functional groups considered in this work, only those containing $–NH_2$ and $–C_4H_3S$ lead to significant hydrosilylation-induced changes in the gap between the highest occupied molecular orbital (HOMO) and the lowest unoccupied molecular orbital (LUMO) of an Si NC at the ground state. The quantum confinement effect is dominant for all of the alkene-hydrosilylated Si NCs at the ground state. At the excited state, the prevailing effect of surface chemistry only occurs at the smallest (0.8 nm) Si NCs hydrosilylated with alkenes containing $–NH_2$ and $–C_4H_3S$. Although the alkyne hydrosilylation gives rise to a more significant surface chemistry effect than alkene hydrosilylation, the quantum confinement effect remains dominant for alkyne-hydrosilylated Si NCs at the ground state. However, at the excited state, the effect of surface chemistry induced by the hydrosilylation with conjugated alkynes is strong enough to prevail over that of quantum confinement.

Keywords: silicon nanocrystals, hydrosilylation, quantum confinement, surface chemistry

PACS: 61.46.Hk, 71.15.Mb, 12.38.Aw, 47.55.dr **DOI:** 10.1088/1674-1056/23/7/076102

1. Introduction

It is well known that the properties of semiconductor nanostructures are often dependent on their sizes.[1–10] One of the most prominent examples of this is the confinement of electrons and holes in a silicon nanocrystal (Si NC) with a size smaller than the Bohr radius of an exciton (~ 5 nm), leading to the bandgap of the Si NC being larger than that of bulk Si.[11–14] This so-called quantum confinement effect has been evidenced for Si NCs synthesized by all kinds of approaches.[15–22] The rather small size of a Si NC also greatly enhances the sensitivity of the electrons/holes of the NC to the NC surface, given a very large ratio of surface area to volume for the NC. It has been found that both inorganic and organic species at the NC surface may indeed impact the electronic and optical properties of Si NCs, signifying the critical role of the surface chemistry.[23–34] Previous works have shown that both quantum confinement and surface chemistry need to be taken into account in the analysis of the properties of Si NCs with inorganic species, such as O and F at the NC surface.[35–40] Wang *et al.* have recently systematically investigated the effect of hydrosilylation-induced organic species at the NC surface on the electronic and optical properties of 1.4 nm Si NCs by using models that closely simulate the experimentally obtained Si NCs.[41] Although the importance of hydrosilylation-induced surface chemistry for Si NCs was highlighted, the interplay between surface chemistry and quantum confinement for hydrosilylated Si NCs was not examined.

In this work, we investigate hydrosilylated Si NCs in the size range from 0.8 nm to 1.6 nm in the framework of density functional theory (DFT). The size variation enables the manifestation of the quantum confinement effect for these Si NCs. Both alkenes and alkynes with a variety of functional groups are considered for the hydrosilylation of Si NCs. The names and formulas of alkenes and alkynes considered in this work are listed in Table 1. The resulting hydrosilylation-induced surface chemistry facilitates a comprehensive evaluation on the interplay between surface chemistry and quantum confinement for hydrosilylated Si NCs. We clearly show that the quantum confinement effect is dominant for all of the alkene/alkyne-hydrosilylated Si NCs at the ground state. For the alkene-hydrosilylated Si NCs at the excited state, the prevailing effect of surface chemistry only occurs at the smallest (0.8 nm) Si NCs hydrosilylated with alkenes containing $–NH_2$ and $–C_4H_3S$. The effect of surface chemistry induced by the hydrosilylation with conjugated alkynes is strong enough to prevail over that of quantum confinement for Si NCs at the excited state.

*Project supported by the National Basic Research Program of China (Grant No. 2013CB632101), the National Natural Science Foundation of China for Excellent Young Researchers (Grant No. 61222404), the Research and Development Program of Ministry of Education of China (Grant No. 62501040202), and the 2012 UAlberta MOST Joint Research Laboratories Program, China.

†Corresponding author. E-mail: mseyang@zju.edu.cn

© 2014 Chinese Physical Society and IOP Publishing Ltd

Table 1. Names and formulas of alkenes and alkynes considered in this work.

	Name	Molecular formula
Alkenes	1-propylene	CH_2=CH–CH_3
	ethenol	CH_2=CH–OH
	acrylic acid	CH_2=CH–COOH
	vinylamine	CH_2=CH–NH_2
	styrene	CH_2=CH–C_6H_5
	2-ethenylpyridine	CH_2=CH–C_5H_4N
	2-ethenylthiophene	CH_2=CH–C_4H_3S
Alkynes	allylene	CH≡C–CH_3
	ethynol	CH≡C–OH
	propiolic acid	CH≡C–COOH
	ethynamine	CH≡C–NH_2
	phenylacetylene	CH≡C–C_6H_5
	2-ethynylpyridine	CH≡C–C_5H_4N
	2-ethynylthiophene	CH≡C–C_4H_3S

2. Model and method

A Si NC is constructed by cutting out the spherical portion from an optimized bulk Si model.[42,43] A Si atom at the NC surface is passivated by one, two, or three hydrogen (H) atoms. Si^A, Si^B, and Si^C are used to denote the Si atoms that are passivated by one, two, and three H atoms at the NC surface, respectively. Alkenes and alkynes with different functional groups (–CH_3, –OH, –COOH, –NH_2, –C_6H_5, –C_5H_4N, –C_4H_3S) are employed to hydrosilylate Si NCs. Recent works have shown that the bonding between Si^C and the exterior alkene/alkyne carbon (C^α) is thermodynamically favored during hydrosilylation.[41,44,45] The length and the coverage of a type of alkyl/alkenyl ligand hardly affect the energies of the highest occupied molecular orbital (HOMO) and the lowest unoccupied molecular orbital (LUMO) of a Si NC, and the HOMO–LUMO gap of the Si NC at both the ground and the excited states.[41] Therefore, we attach one ligand derived from a model alkene/alkyne molecule in the form of H_2C=CHX/HC≡CX (X = CH_3, OH, COOH, NH_2, C_6H_5, C_5H_4N, or C_4H_3S) to the NC surface via the bonding of Si^C–C^α.

Our calculation is performed by using the modeling program of DMol3. The Becke–Lee–Yang–Parr (BLYP) exchange–correlation function at the generalized gradient approximation (GGA) level in the frame of all-electron density functional theory is used.[46] Double numerical basis sets augmented with p-polarization functions (DNP basis sets) are used as the atomic orbital basis functions. In the DNP basis sets, the orbital cutoff radius is 0.47 nm. In order to ensure accurate calculations, we have selected a high self-consistent field (SCF) convergence threshold (10^{-6}). The maximum forces on all of the atoms in the optimized Si NCs are less than 0.05 eV/Å. The spin polarization is included to determine the spin multiplicities for Si NCs at both the ground and the excited states. The HOMO–LUMO gap of the Si NC at the ground state is readily calculated once the structural and electronic optimization of the NC is finished.

The excited state of the Si NC is initiated by moving an electron in the HOMO to the LUMO and leaving a hole in the HOMO. The structural and electronic optimization is then carried out. We find that the optimization for a 1.2/1.6 nm Si NC hydrosilylated with vinylamine and a 1.6 nm Si NC hydrosilylated with 2-ethenylthiophene at the excited state cannot be converged. However, the resulting absence of certain data should not prevent us from drawing conclusions by means of a comprehensive analysis. Please note that the HOMO–LUMO gaps reported in this work are underestimated by ∼ 1–2 eV because of the BLYP-based DFT employed in this work.[1] However, the relative order among the HOMO–LUMO gaps is not affected by the underestimation. We calculate the percentage of the HOMO (LUMO) density residing at a ligand at the surface of a hydrosilylated Si NC by the C-squared population analysis (CSPA) method. The sum of squares of molecular orbital (MO) coefficients from all the elements in the hydrosilylated Si NC (S_w) and that from the elements in the ligand (S_l) are first calculated. The ratio of the resulting two values (S_l/S_w) is the percentage of the HOMO (LUMO) density residing at the ligand. Please note that the HOMO (LUMO) density residing at the H atoms in the ligand is not included in S_l. Hence, the percentage of the HOMO (LUMO) density residing at the ligand is somewhat underestimated.

3. Results and discussion

3.1. Alkene-hydrosilylated Si NCs

Figure 1 shows the HOMO energy, the LUMO energy, and the HOMO–LUMO gap of an alkene-hydrosilylated Si NC at the ground state. The NC size changes from 0.8 nm to 1.6 nm. Si NCs with full hydrogen passivation (FHP) are also incorporated for comparison. As the size of the fully H-passivated Si NC decreases, its HOMO decreases (Fig. 1(a)) and LUMO increases (Fig. 1(b)). This leads to the increase in the HOMO–LUMO gap of the Si NC with the decrease of the NC size, which is consistent with the quantum confinement effect. It is clear that the alkene hydrosilylation does not affect the LUMO energy. Except the hydrosilylation with alkenes containing –NH_2 and –C_4H_3S, the alkene hydrosilylation considered here hardly affects the HOMO energy. Therefore, we can see that the dependence of the HOMO–LUMO gap on the NC size for the Si NCs hydrosilylated with alkenes that do not contain –NH_2 and –C_4H_3S is basically similar to that for the fully H-passivated Si NCs.

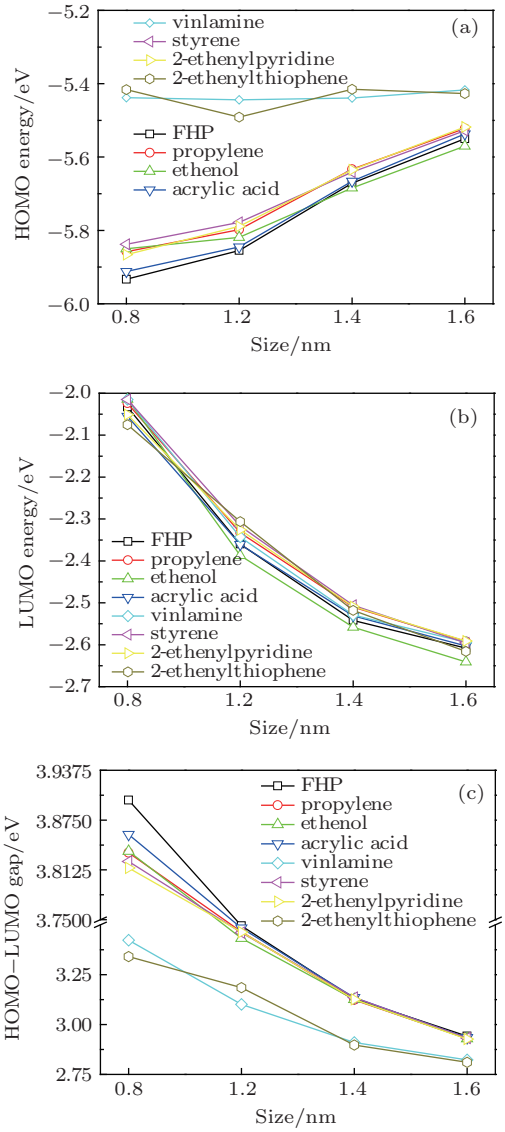


Fig. 1. (color online) (a) The HOMO energy, (b) the LUMO energy, and (c) the HOMO–LUMO gap of alkene-hydrosilylated (propylene, ethenol, acrylic acid, vinlamine, styrene, 2-ethenylpyridine, and 2-ethenylthiophene) and fully H-passivated (FHP) Si NCs in the size range from 0.8 nm to 1.6 nm at the ground state.

Figure 2 representatively shows the distributions of the electron wave functions of the HOMO and the LUMO for 0.8 nm and 1.4 nm fully H-passivated Si NCs and those hydrosilylated with propylene ($-CH_3$), vinylamine ($-NH_2$), and 2-ethenylthiophene ($-C_4H_3S$) at the ground state. The percentages of the HOMO/LUMO density residing at the ligands are listed in Table 2. It is found that both HOMO and LUMO are mainly located inside the Si NC when it is hydrosilylated with propylene ($-CH_3$), ethanol (–OH), acrylic acid (–COOH), and styrene ($-C_6H_5$) (only the case for propylene hydrosilylation is shown in Fig. 2 and Table 2), similar to that in the fully H-passivated Si NC. However, the HOMO is significantly localized at the ligand ($> 80\%$ of the HOMO density) when an Si NC is hydrosilylated with vinylamine and 2-ethenylthiophene. It is this localization that leads to the increase in the HOMO energy for the Si NC hydrosilylated with vinylamine and 2-ethenylthiophene (Figs. 1(a) and 1(b)). In fact, the localization of the HOMO at the ligand derived from vinylamine or 2-ethenylthiophene results in little change of the HOMO energy with the variation of the NC size. However, the increasing trend for the HOMO–LUMO gap with the decrease of the NC size for the vinylamine- or 2-ethenylthiophene-hydrosilylated Si NC is maintained because the hydrosilylation does not affect the increase of the LUMO energy with the decrease of the NC size. This means that the quantum confinement effect remains dominant.

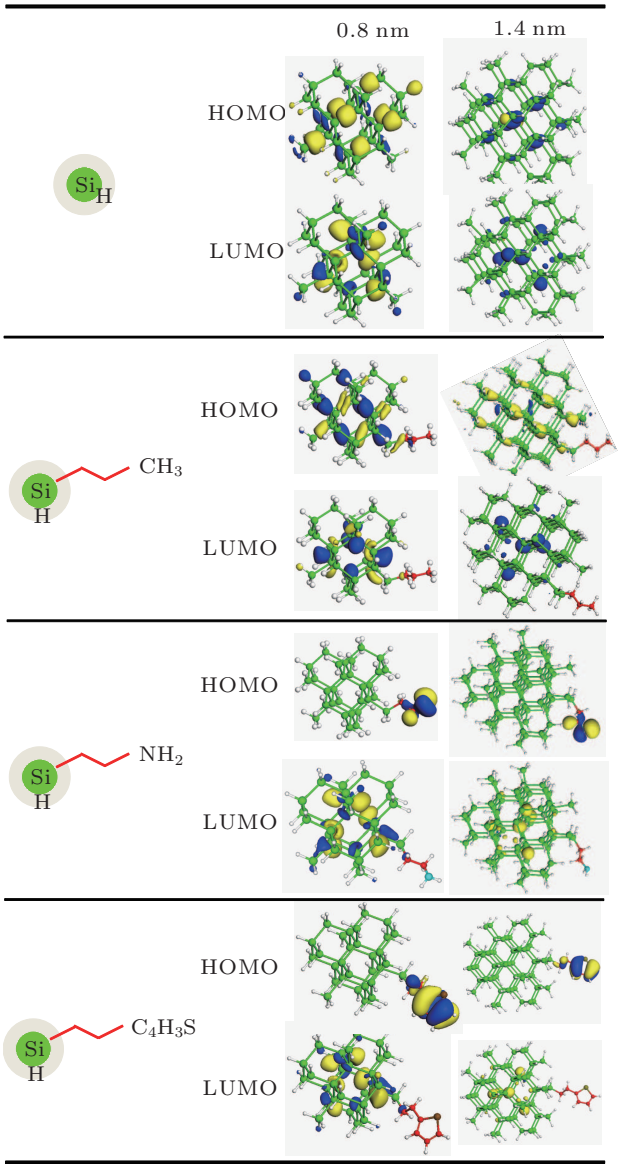


Fig. 2. (color online) Distributions of the electron wave functions of the HOMO and the LUMO for 0.8 nm and 1.4 nm fully H-passivated Si NCs and those hydrosilylated with propylene ($-CH_3$), vinylamine ($-NH_2$) and 2-ethenylthiophene ($-C_4H_3S$) at the ground state. Si, C, N, S, and H atoms are denoted by green, red, cyan, dark yellow, and white balls, respectively.

Figure 3 shows the HOMO energy, the LUMO energy, and the HOMO–LUMO gap of alkene-hydrosilylated and fully H-passivated Si NCs in the size range from 0.8 nm

to 1.6 nm at the excited state. As shown before, the quantum confinement in extremely small Si NCs may be seriously weakened at the excited state.[36] The weakened quantum confinement results in the increase in the HOMO energy and the decrease in the LUMO energy (Figs. 3(a) and 3(b)). Thus, the HOMO–LUMO gap decreases when the size of the fully H-passivated Si NC decreases from 1.4 nm to 0.8 nm (Fig. 3(c)). The percentages of the HOMO/LUMO density residing at the ligands are also listed in Table 2. The percentages of the HOMO/LUMO density residing at the ligands of the 1.4 nm Si NC hydrosilylated with any alkenes are less than 0.1 %. This leads to rather small changes in the HOMO energy, the LUMO energy and thus the HOMO–LUMO gap for the 1.4 nm Si NC after alkene-hydrosilylation. The changes will diminish as the NC size increases (e.g., 1.6 nm). However, the changes are enlarged when the NC size decreases to 1.2 nm and 0.8 nm. This is due to the transfer of the HOMO and the LUMO to the ligands for small hydrosilylated Si NCs, evidenced by the increase of the percentage of the HOMO/LUMO density residing at the ligand as the NC size decreases from 1.4 nm to 0.8 nm (Table 2). For the 0.8-nm Si NC hydrosilylated with the alkene containing $–C_4H_3S$, the localization of the HOMO/LUMO at the ligands is so significant that the HOMO/LUMO energy is enormously changed. This gives rise to a large increase of the HOMO–LUMO gap with the decrease of the NC size from 1.2 nm to 0.8 nm. We find that the HOMO/LUMO energy and thus the HOMO–LUMO gap are also significantly changed for the 0.8-nm Si NC hydrosilylated with vinylamine ($–NH_2$), although both the HOMO and the LUMO are only slightly transferred to the ligand. These changes are actually due to the improved quantum confinement, as evidenced by the increased distribution of the electron wavefunction of the HOMO/LUMO under the surface Si atoms. The underlying mechanism for the enhancement of the quantum confinement by vinylamine for a very small (0.8 nm) Si NC needs further investigation. The fact that with the decrease of the NC size from 1.2 nm to 0.8 nm, the change of the HOMO–LUMO gap for the Si NC hydrosilylated with vinylamine ($–NH_2$) or 2-ethenylthiophene ($–C_4H_3S$) is contrary to that for the fully H-passivated Si NC indicates that the effect of surface chemistry induced by the hydrosilylation with alkenes containing $–NH_2$ and $–C_4H_3S$ prevails over that of quantum confinement for the 0.8 nm Si NCs at the excited state.

Table 2. Percentages of the HOMO/LUMO density residing at the ligands for 0.8-nm and 1.4-nm Si NCs hydrosilylated with propylene, vinylamine, and 2-ethenylthiophene at the ground and the excited states.

		HOMO/%			LUMO/%		
		$–CH_3$	$–NH_2$	$–C_4H_3S$	$–CH_3$	$–NH_2$	$–C_4H_3S$
Ground state	0.8 nm	3.95	81.48	91.12	0.96	0.84	1.34
	1.4 nm	0.80	81.08	94.78	0.09	0.09	0.28
Excited state	0.8 nm	0.92	8.41	92.61	0.69	0.28	66.04
	1.4 nm	0.51	2.18	3.49	0.01	0.01	0.01

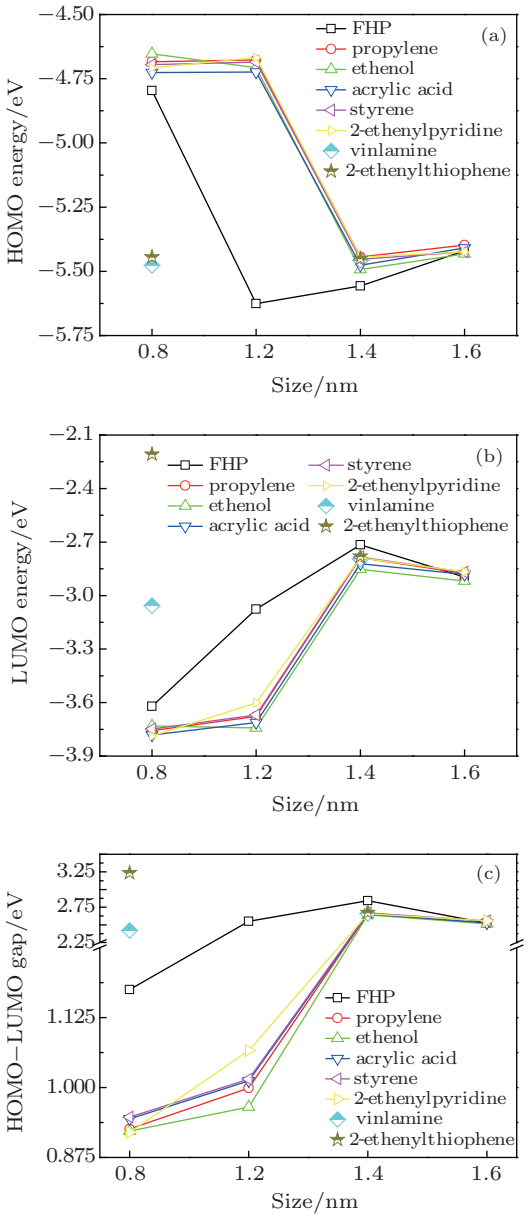


Fig. 3. (color online) (a) The HOMO energy, (b) the LUMO energy, and (c) the HOMO–LUMO gap of alkene-hydrosilylated (propylene, ethenol, acrylic acid, vinlamine, styrene, 2-ethenylpyridine, 2-ethenylthiophene) and fully H-passivated Si NCs in the size range from 0.8 nm to 1.6 nm at the excited state.

3.2. Alkyne-hydrosilylated Si NCs

The HOMO energy, the LUMO energy, and the HOMO–LUMO gap of an alkyne-hydrosilylated or fully H-passivated Si NC in the size range from 0.8 nm to 1.6 nm at the ground state are shown in Fig. 4. Except for propiolic acid, the alkynes considered in this work lead to the hydrosilylation-induced changes in the HOMO energy being larger than those in the LUMO energy. The distributions of the electron wave functions of the HOMO and the LUMO for 0.8-nm and 1.4-nm fully H-passivated Si NCs and those hy-

drosilylated with allylene, propiolic acid, ethynamine, and 2-ethynylthiophene are representatively shown in Fig. 5. The percentages of the HOMO/LUMO density residing at the ligands are also listed in Table 3. The transfer of the HOMO to the ligands causes the increases of the HOMO energy for the Si NCs hydrosilylated with allylene, ethynol, ethynamine, phenylacetylene, 2-ethynylpyridine, and 2-ethynylthiophene, while the transfer of the LUMO to the propiolic-acid-derived ligand leads to the decrease of the LUMO energy for the propiolic-acid-hydrosilylated Si NC. In spite of all of the changes, the HOMO–LUMO gap of the alkyne-hydrosilylated Si NC still increases with the decrease of the NC size. This indicates the dominant

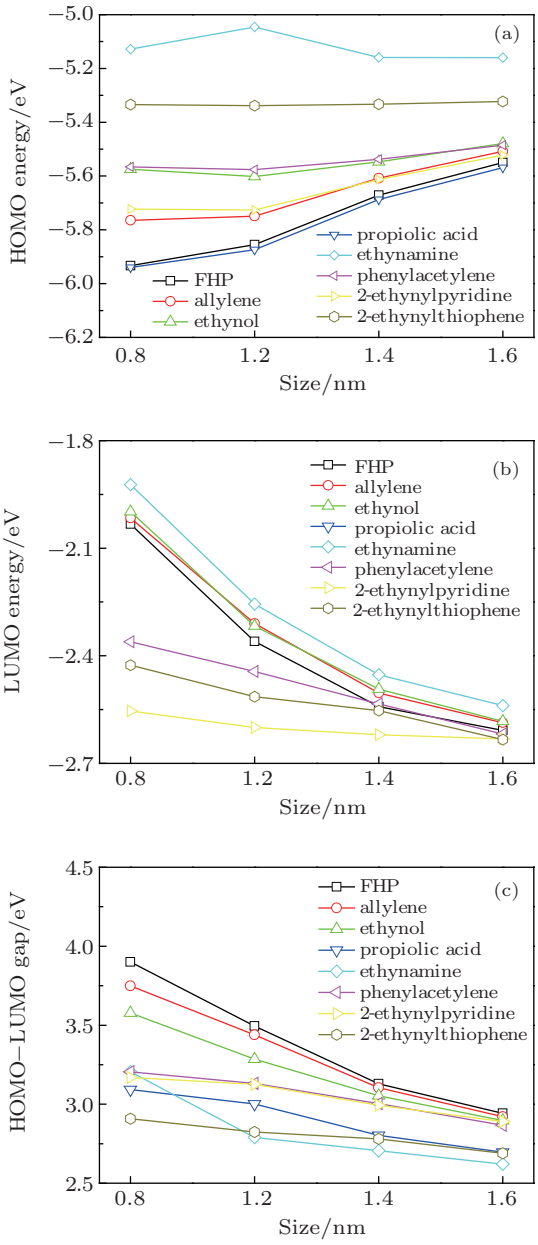


Fig. 4. (color online) (a) The HOMO energy, (b) the LUMO energy, and (c) the HOMO–LUMO gap of alkyne-hydrosilylated (allylene, ethynol, propiolic acid, ethynamine, phenylacetylene, 2-ethynylpyridine, 2-ethynylthiophene) and fully H-passivated Si NCs in the size range from 0.8 nm to 1.6 nm at the ground state.

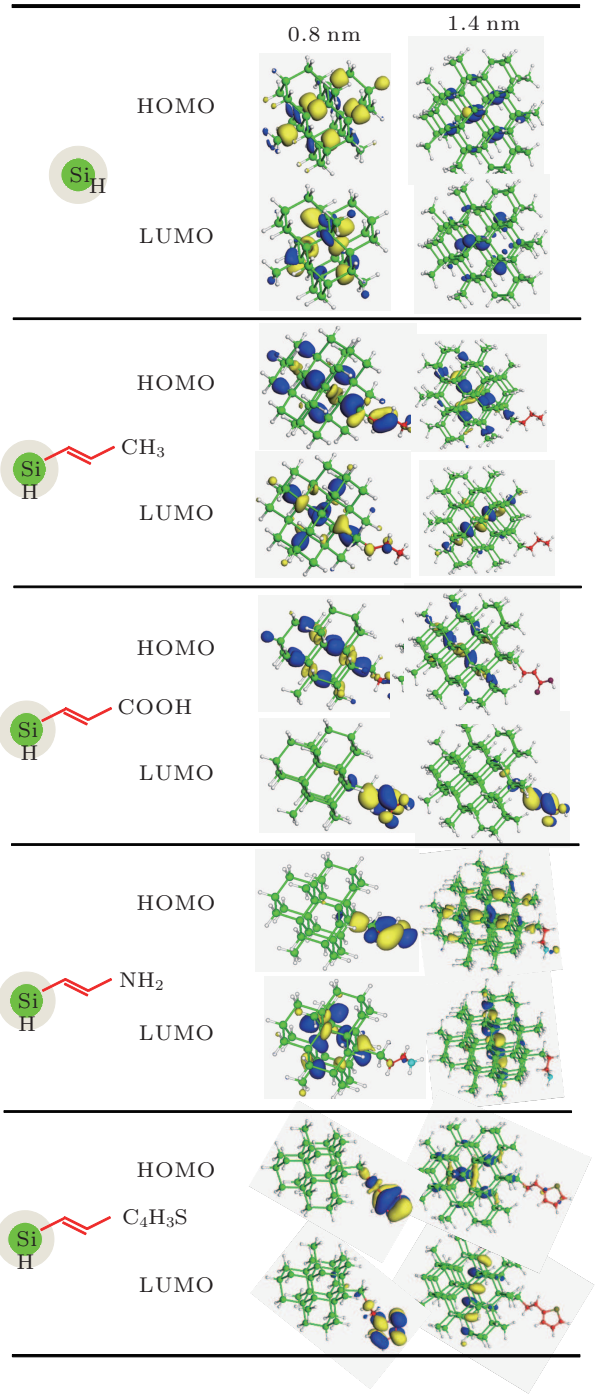


Fig. 5. (color online) Distributions of the electron wave functions of the HOMO and the LUMO for 0.8-nm and 1.4-nm fully H-passivated Si NCs and those hydrosilylated with allylene (–CH_3), propiolic acid (–COOH), ethynamine (–NH_2), and 2-ethynylthiophene (–C_4H_3S) at the ground state. Si, C, O, N, S, and H atoms are denoted by green, red, purple, cyan, dark yellow, and white balls, respectively.

role of quantum confinement for the alkyne-hydrosilylated Si NCs at the ground state.

Figure 6 shows the distributions of electron density for: (a) a 0.8 nm Si NC hydrosilylated with propiolic acid, (b) a 1.2 nm Si NC hydrosilylated with propiolic acid (–COOH), (c) a 0.8 nm Si NC hydrosilylated with ethynol (–OH), and (d) a 0.8 nm Si NC hydrosilylated with ethynamine (–NH_2) at the excited state. It is seen that the back bond of Si–C (i.e.,

1-2 Si-Si bond) is significantly elongated in each case. The electron densities at the 1–2 Si–Si bonds are extremely small. This means that the ligands may actually be detached from the NC surface when these Si NCs are excited. Therefore, their corresponding data for the HOMO/LUMO energies and the HOMO–LUMO gaps are voided.

Table 3. Percentages of the HOMO/LUMO density residing at the ligands for 0.8-nm and 1.4-nm Si NCs hydrosilylated with allylene (–CH_3), propiolic acid (–COOH), ethynamine (–NH_2), and 2-ethynylthiophene (–C_4H_3S) at the ground state. Percentages of the HOMO/LUMO density residing at the ligands for 0.8-nm and 1.4-nm Si NCs hydrosilylated with allylene (–CH_3), phenylacetylene (–C_6H_5), 2-ethynylpyridine (–C_5H_4N), and 2-ethynylthiophene (–C_4H_3S) at the excited state.

		HOMO/%		LUMO/%	
		0.8 nm	1.4 nm	0.8 nm	1.4 nm
Ground state	–CH_3	13.42	3.24	2.00	0.22
	–COOH	4.94	0.80	71.56	58.78
	–NH_2	72.65	71.73	1.04	0.20
	–C_4H_3S	80.67	78.31	69.16	15.15
Excited state	–CH_3	5.71	1.94	4.20	0.08
	–C_6H_5	66.87	60.76	66.47	54.33
	–C_5H_4N	62.63	55.36	68.92	57.16
	–C_4H_3S	76.70	75.29	75.10	67.35

Figure 7 shows the available HOMO energy, LUMO energy, and HOMO–LUMO gap of the alkyne-hydrosilylated Si NC in the size range from 0.8 nm to 1.6 nm at the excited state. The fully H-passivated Si NCs are also considered for comparison. We now focus on the hydrosilylation with conjugated alkynes (i.e., phenylacetylene, 2-ethynylpyridine, and 2-ethynylthiophene), since the changes in the HOMO energy, the LUMO energy, and the HOMO–LUMO gap induced by the hydrosilylation with other alkynes are basically similar to those for the case of alkene hydrosilylation. By examining the distributions of the electron wave functions of the HOMO and the LUMO and the percentages of the HOMO/LUMO density residing at the ligand for the conjugated-alkyne-hydrosilylated Si NC (Table 3), we find that both the HOMO and the LUMO are significantly localized at the ligand for the Si NC hydrosilylated with a conjugated alkyne, regardless of the NC size. Hence, the HOMO and the LUMO are characteristic of the conjugated-alkyne-derived ligand. This explains that the HOMO energy and the LUMO energy hardly change with the varying size of the conjugated-alkyne-hydrosilylated Si NC, disabling the dependence of the HOMO–LUMO gap on the NC size. It is apparent here that the effect of surface chemistry induced by the hydrosilylation with conjugated alkynes prevails over that of quantum confinement.

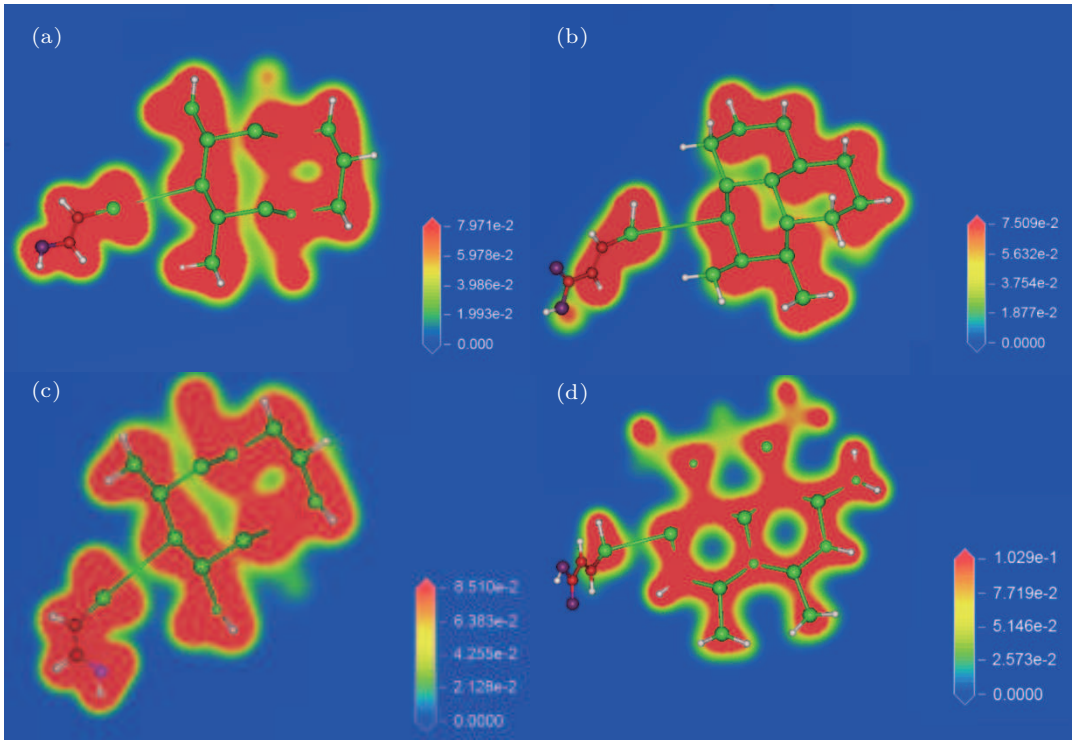


Fig. 6. (color online) Distributions of electron density for: (a) 0.8-nm Si NC hydrosilylated with propiolic acid, (b) 1.2-nm Si NC hydrosilylated with propiolic acid, (c) 0.8-nm Si NC hydrosilylated with ethynol, and (d) 0.8-nm Si NC hydrosilylated with ethynamine. All the hydrosilylated Si NCs are at the excited state. Si, C, O, N, and H atoms are denoted by green, red, purple, dark yellow, and white balls, respectively.

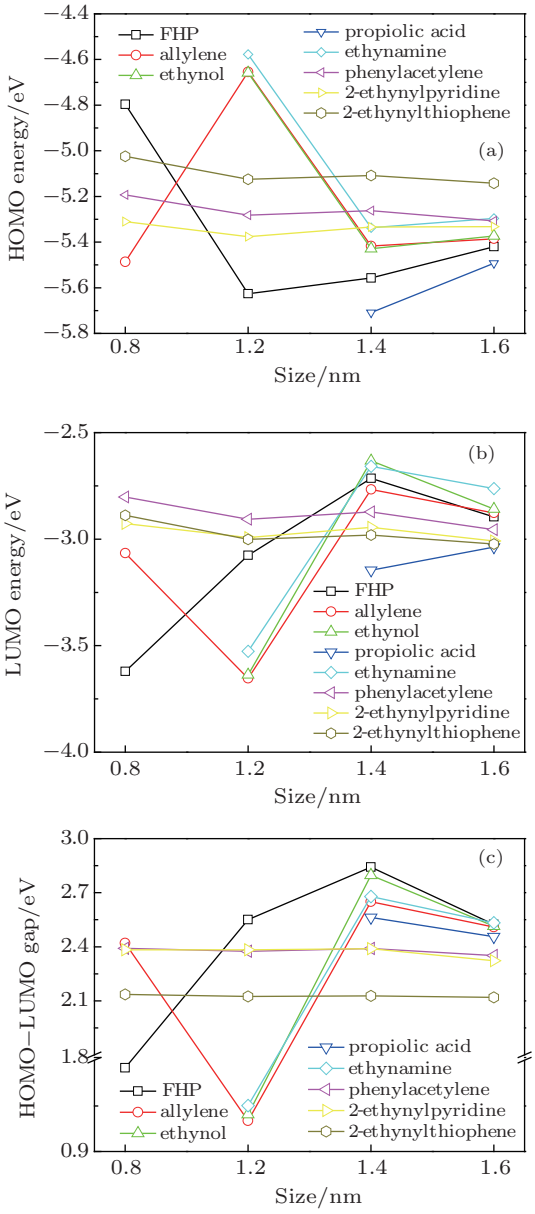


Fig. 7. (color online) (a) The HOMO energy, (b) the LUMO energy, and (c) the HOMO–LUMO gap of alkyne-hydrosilylated (allylene, ethynol, propiolic acid, ethynamine, phenylacetylene, 2-ethynylpyridine, 2-ethynylthiophene) and fully H-passivated Si NCs in the size range from 0.8 nm to 1.6 nm at the excited state.

4. Conclusion

The electronic properties of hydrosilylated Si NCs in the size range from 0.8 nm to 1.6 nm have been investigated by means of DFT. The interplay between quantum confinement and hydrosilylation-induced surface chemistry for Si NCs is manifested on the changes in the HOMO/LUMO energy and the HOMO–LUMO gap. We find that alkenes containing the functional groups of $–NH_2$ and $–C_4H_3S$ lead to significant hydrosilylation-induced changes in the HOMO–LUMO gap of the Si NC at the ground state. For all the alkene-hydrosilylated Si NCs at the ground state, the quantum confinement effect is dominant. At the excited state, the prevailing effect of surface chemistry only occurs to the smallest (0.8 nm) Si NCs hydrosilylated with alkenes containing the functional groups of $–NH_2$ and $–C_4H_3S$. The quantum confinement effect is also dominant for alkyne-hydrosilylated Si NCs at the ground state. However, at the excited state, the effect of surface chemistry induced by the hydrosilylation with conjugated alkynes prevails over that of quantum confinement. The current results should contribute to the design and optimization of hydrosilylation schemes for the processing of the originally H-passivated Si NCs that are routinely produced in experiments.

Acknowledgments

We thank Prof. Jonathan G. C. Veinot and Mr. Zhenyu Yang at the University of Alberta for the discussion on the hydrosilylation of Si NCs. Shanghai Supercomputer Center is thanked for providing the computation resources.

References

[1] Williamson A J, Grossman J C, Hood R Q, Puzder A and Galli G 2002 *Phys. Rev. Lett.* **89** 196803
[2] Pi X D, Liptak R W, Nowak J D, Pwells N, Carter C B, Campbell S A and Kortshagen U 2008 *Nanotechnology* **19** 245603
[3] Nunez J R R, Kelly J A, Henderson E J and Veinot J G C 2012 *Chem. Mater.* **24** 346
[4] Zhang X H, Dong J C, Wang Y, Li L and Li H 2013 *J. Phys. Chem. C* **117** 12958
[5] Mastronardi M L, Maier-Flaig F, Faulkner D, Henderson E J, Kübel C, Lemmer U and Ozin G A 2012 *Nano Lett.* **12** 337
[6] Dong J C and Li H 2012 *J. Phys. Chem. C* **116** 17259
[7] Hua F J, Swihart M T and Ruckenstein E 2005 *Langmuir* **21** 6054
[8] Ledoux G, Guillois O, Porterat D, Reynaud C, Huisken F, Kohn B and Paillard V 2000 *Phys. Rev. B* **62** 15942
[9] Kovalev D and Fujii M 2005 *Adv. Mater.* **17** 2531
[10] Ni Z Y, Pi X D and Yang D 2012 *Chin. Phys. Lett.* **29** 077801
[11] Vasiliev I, Öğüt S and Chelikowsky J R 2001 *Phys. Rev. Lett.* **86** 1813
[12] Cullis A 1997 *J. Appl. Phys.* **82** 909
[13] Delerue C, Allan G and Lannoo M 1993 *Phys. Rev. B* **48** 11024
[14] Zunger A and Wang L W 1996 *Appl. Surf. Sci.* **102** 350
[15] Kortshagen U 2009 *J. Phys. D: Appl. Phys.* **42** 113001
[16] Veinot J G C 2006 *Chem. Commun.* 4160
[17] Li X G, He Y Q, Talukdar S S and Swihart M T 2003 *Langmuir* **19** 8490
[18] Bley R A and Kauzlarich S M 1996 *J. Am. Chem. Soc.* **118** 12461
[19] Pi X D, Zalloum O H Y, Wojcik J, Knights A P, Mascher P, Todd A D W and Simpson P J. 2005 *J. Appl. Phys.* **97** 096108
[20] Gresback R, Nozaki T and Okazaki K 2011 *Nanotechnology* **22** 305605
[21] Gupta A, Swihart M T and Wiggers H 2009 *Adv. Funct. Mater.* **19** 696
[22] Mastronardi M L, Henderson E J, Puzzo D P and Ozin G A 2012 *Adv. Mater.* **24** 5890
[23] Martínez A, Alonso J C, Sansores L E and Salcedo R 2010 *J. Phys. Chem. C* **114** 12427
[24] Zhou Z, Brus L and Friesner R 2003 *Nano Lett.* **3** 163
[25] Reboredo F A, Schwegler E and Galli G 2003 *J. Am. Chem. Soc.* **125** 15243
[26] Pi X D 2012 *J. Nanomater.* **2012** 912903
[27] Ma Y S, Chen X B, Pi X D and Yang D 2011 *J. Phys. Chem. C* **115** 12822
[28] Zhang R Q, Li Q S, Lee S T, Niehaus T A and Frauenheim T 2008 *J. Chem. Phys.* **128** 244714
[29] Puzder A, Williamson A J, Grossman J C and Galli G 2002 *Phys. Rev. Lett.* **88** 097401
[30] Chao Y, Houlton A, Horrocks B R, Hunt M R C, Poolton N R J, Yang J and Siller L 2006 *Appl. Phys. Lett.* **88** 263119

[31] Coxon P R, Wang Q and Chao Y 2011 *J. Phys. D: Appl. Phys.* **44** 495301

[32] Belomoin G, Rogozhina E, Therrien J, Braun P V, Abuhassan L, Nayfeh M H, Wagner L and Mitas L 2002 *Phys. Rev. B* **65** 193406

[33] Puzder A, Williamson A J, Grossman J C and Galli G 2002 *J. Chem. Phys.* **117** 6721

[34] He Y, Su Y, Yang X, Kang Z, Xu T, Zhang R, Fan C and Lee S T 2009 *J. Am. Chem. Soc.* **131** 4434

[35] Chen X B, Pi X D and Yang D 2010 *J. Phys. Chem. C* **114** 8774

[36] Ma Y S, Pi X D and Yang D 2012 *J. Phys. Chem. C* **116** 5401

[37] Wolkin M V, Jorne J, Fauchet P M, Allan G and Delerue C 1999 *Phys. Rev. Lett.* **82** 197

[38] Gole J L, Veje E, Egeberg R G, Ferreira da Silva A, Pepe I and Dixon D A 2006 *J. Phys. Chem. B* **110** 2064

[39] Qin C J, Huang W Q, Wang H X and Jin F 2008 *Chin. Phys. B* **17** 3753

[40] Liu S R, Qin C J, Huang W Q, Xu L, Wang H X, Jin F, Wu K Y and Qin S J 2008 *Chin. Phys. B* **17** 1817

[41] Wang R, Pi X D and Yang D 2012 *J. Phys. Chem. C* **116** 19434

[42] Chen X B, Pi X D and Yang D 2011 *J. Phys. Chem. C* **115** 661

[43] Pi X D, Chen X B, Ma Y S and Yang D 2011 *Nanoscale* **3** 4584

[44] Jariwala B N, Dewey O S, Stradins P, Ciobanu C V and Agarwal S 2011 *ACS Appl. Mater. Inter.* **3** 3033

[45] Calder S, Boies A, Lei P Y, Girshick S and Roberts J 2011 *Chem. Mater.* **23** 2917

[46] Pi X D, Chen X B and Yang D 2011 *J. Phys. Chem. C* **115** 9838